Laser and Particle Beams (2015), *33*, 193–200.

doi:10.1017/S026303461500021X

Low temperature photoionized Ne plasmas induced by laser-plasma EUV sources

A. BARTNIK, H. FIEDOROWICZ, T. FOK, R. JAROCKI, M. SZCZUREK, AND P. WACHULAK
Institute of Optoelectronics, Military University of Technology, Warsaw, Poland

(RECEIVED 17 October 2014; ACCEPTED 9 February 2015)

Abstract

In this work, two laser-produced plasma (LPP) sources – extreme ultraviolet (EUV) and a LPP soft X-ray (SXR) source were used to create Ne photoionized plasmas. A radiation beam was focused onto a gas stream, injected into a vacuum chamber synchronously with the radiation pulse. EUV radiation spanned a wide spectral range with pronounced maximum centered at $\lambda \approx 11$ nm, while in case of the SXR source spectral maximum was at $\lambda \approx 1.4$ nm. Emission spectra of photoionized plasmas created this way were measured in a wide spectral range $\lambda = 10$–100 nm. The dominating spectral lines originated from singly charged ions (Ne II) and neutral atoms (Ne I). For the highest radiation fluence, spectral lines originating from Ne III and even Ne IV species were detected. Differences between the experimental spectra, obtained for all irradiation conditions, were analyzed. They were attributed either to different fluence or spectral distribution of driving photons.

Keywords: Extreme ultraviolet; Laser plasma; Photoionization; Soft X rays

1. INTRODUCTION

X-ray and extreme ultraviolet (EUV) photons carry enough energy to ionize any atom or molecule. Interaction of this kind of photons with matter results in releasing of photoelectrons usually having energies sufficient for further ionization or excitation. In case of solids the radiationless recombination may cause defects and chemical changes in irradiated material. If the radiation power density is high enough, ablation of the material can occur. Such phenomenon was demonstrated in various experiments using synchrotrons (Zhang *et al*., 1995), free electron lasers (FEL) (Juha *et al*., 2003), or laser-produced-plasma (LPP) sources (Bartnik *et al*., 2005; Makimura *et al*., 2005;). In case of FEL the power density and energy fluence is usually sufficiently high for multiple ionization of the ablated material and formation of non-equilibrium plasma. Plasma formation by X-ray irradiation of solids is also possible using the so-called high-energy-density (HED) facilities (Perry *et al*., 1996). Extremely high-energy X-ray pulses, produced in these installations, are used for example for fusion experiments (Hurricane *et al*., 2014).

High-power X-ray sources can be used also for plasma production in gaseous media. In this case photoionization results in direct conversion of gaseous media into photoionized plasmas. In contrary to interaction with solids no energy is lost for material ablation, thus plasma can be formed with much lower radiation intensity. Experiments on photoionized plasmas produced by irradiation of gases using high-power X-ray sources concern the so-called laboratory astrophysics. The term refers to experimental simulation of some processes or forms of matter present in the Space. Most of the matter in the Universe is ionized due to heating by gravitational compression or exposure to intense EUV or X-ray radiation. Photoionization of gases is a key process in the formation of different kinds of astrophysical plasmas, especially located close to strongly radiating compact objects. Photoionized plasmas of corresponding parameters were investigated in series of experiments using high-power X-ray pulses, produced in high-power laser facilities GEKKO XII (Fujioka *et al*., 2009) and Shenguang II (Wei *et al*., 2008) or the *Z*-pulsed-power facility (Bailey *et al*., 2001; Cohen *et al*., 2003). In these experiments, the irradiated media were placed close to the X-ray radiating plasmas. X-ray power densities in the extreme cases exceeded 10^{11} W/cm^2 and were sufficient for the formation of photoionized plasmas with high ionization degree. A brief review of interpretation of astrophysical observations, supported by the laboratory

Address correspondence and reprint requests to: A. Bartnik, Military University of Technology, Warsaw, Mazowsze, Poland.
E-mail: andrzej.bartnik@wat.edu.pl

astrophysics experiments, was presented in (Mancini *et al.*, 2009).

Photoionized plasmas are also formed by X-ray or EUV irradiation of interstellar media or outer regions of planetary atmospheres. In the latter case, the EUV radiation is especially important because of strong interaction with valence and core electrons and significant contribution of the EUV in Solar electromagnetic radiation. The EUV radiation ionizes upper planetary atmospheres (Lammer *et al.*, 2011) forming low-density plasmas. Laboratory simulation of this kind of photoionized plasmas does not require extremely high radiation field because of relatively high values of cross-sections for processes induced by EUV photons comparing with X-rays (Watson, 1972; Gallagher *et al.*, 1988; Itikawa *et al.*, 1989; Samson & Stolte, 2002). In this case, photoionized plasmas can be created using EUV radiation pulses of moderate intensity, available from small-scale laboratory sources, at radiation intensity of the order of 10^7-10^9 W/cm^2 (Bartnik *et al.*, 2013*a*; 2013*b*; 2013*c*).

Of course it is not possible to reproduce astrophysical plasmas in laboratory conditions because of different size, density, and temporal evolution. Other parameters, however, like temperature or ionic composition can be achieved. Also, some parameters of radiation field forming the photoionized plasmas in space can be simulated in the laboratory. Investigations of the laboratory plasmas can support accuracy of physical models, constructed for analysis of observed spectra from astrophysical plasmas.

In this work, spectral investigations of Ne photoionized plasmas induced using three different radiation sources, were performed. The sources are based on nanosecond Nd:YAG lasers of different parameters and double-stream gas puff targets. The radiation is focused by EUV or soft X-ray (SXR) collectors. Low-temperature Ne plasmas, composed of mainly neutral atoms and singly charged ions, were produced. Significant influence of radiation intensity and spectral distribution of the driving radiation pulses on ionic composition was demonstrated. For the most intense radiation, Ne III and even Ne IV species were detected. Differences in relative intensities of the most characteristic spectral lines were discussed.

2. EXPERIMENT

2.1. EUV Sources

In our experiments, three LPP, EUV, and SXR sources were used. They were based on Nd:YAG lasers of different parameters and equipped with appropriate focusing collectors. The first one (Source No. 1) was a 10-Hz LPP EUV source, based on a double-stream gas-puff target, irradiated with the 4 ns/0.8 J Nd:YAG laser pulse. The target was created by pulsed injection of a krypton – xenon (90/10%) gas mixture into a hollow stream of helium by employing an electromagnetic valve system, equipped with a double-nozzle setup. The focusing conditions and plasma parameters were adjusted to obtain the maximum intensity in the EUV spectral region. The radiation was focused using a gold-plated grazing incidence ellipsoidal collector, manufactured by Rigaku Innovative Technologies Europe s.r.o., Czech Republic. The collector is a part of an ellipsoid having a collection angle of 0.8 sr. Roughness of its reflective surface is smaller than 1 nm. The collector has a rotational symmetry and plasma is located in one of its focal points. An incidence angle for the focused radiation is approximately 15°. The collector allowed for effective focusing of radiation emitted from Kr/Xe plasma in the wavelength range $\lambda = 9$–70 nm. The most intense emission was in the relatively narrow spectral region, centerd at $\lambda = 11 \pm 1$ nm. The spectral intensity at longer wavelength range was much smaller; however, spectrally integrated intensities in both ranges were comparable. The EUV fluence in a focal plane of the collector reached 0.1 J/cm^2 at the center of a focal spot. A full width half maximum diameter of the intensity distribution in the focal spot was 1.4 mm. Schematic view of the source together with the spectrum of the focused EUV radiation is presented in Figure 1a and 1b. It should be pointed out that short wavelength radiation with the wavelengths below 8 nm is not reflected from the collector surface. Detailed description of the source and parameters of the focused EUV radiation can be found elsewhere (Bartnik *et al.*, 2011).

The second EUV source (Source No .2) was based on a 10 J/10 Hz Nd:YAG laser system with the pulse duration of 10 ns. In this case, also a double-stream gas-puff target was employed for plasma creation. The only difference was that the Kr/Xe mixture was replaced by pure Xe gas. Laser pulse energy in this case could be changed from 1 to 10 J. Increase of the pulse energy resulted in spectral shift of the emitted radiation toward the SXR region. In all cases, however, plasma emission is dominated by the EUV radiation. This part of radiation was collected and focused with good efficiency using a Mo-coated ellipsoidal mirror having the same geometry as the EUV collector used for the Source No. 1. Spectral distribution of the focused EUV radiation, obtained in this case, is presented in Figure 1c. The most intense emission was again in the spectral region close to $\lambda = 11$ nm; however, the spectrum contains the second wide maximum around $\lambda = 16$ nm. Maximum value of the EUV fluence in a focal plane of the collector exceeded 0.4 J/cm^2. Experimental arrangement of the source is similar to the Source No. 1 as shown in Figure 1a.

The third source (Source No. 3) was based on the same laser system as in case of the Source No. 2. In this case, however, the laser pulse was shortened to approximately 1 ns using an Stimulated Brillouin Scattering (SBS) mirror. Also in this case the plasma is being created by a laser irradiation of the double-stream gas-puff target that used Xe gas as the working medium. Plasma radiation spectrum in this case spans the wide wavelength range with strong maximum at $\lambda \approx 1.4$ nm. The radiation was focused using a paraboloidal collector consisting of a set of two identical axisymmetrical paraboloidal mirrors mounted coaxially, as shown in Figure 2a. Plasma is located in a focal point of

https://doi.org/10.1017/S026303461500021X Published online by Cambridge University Press

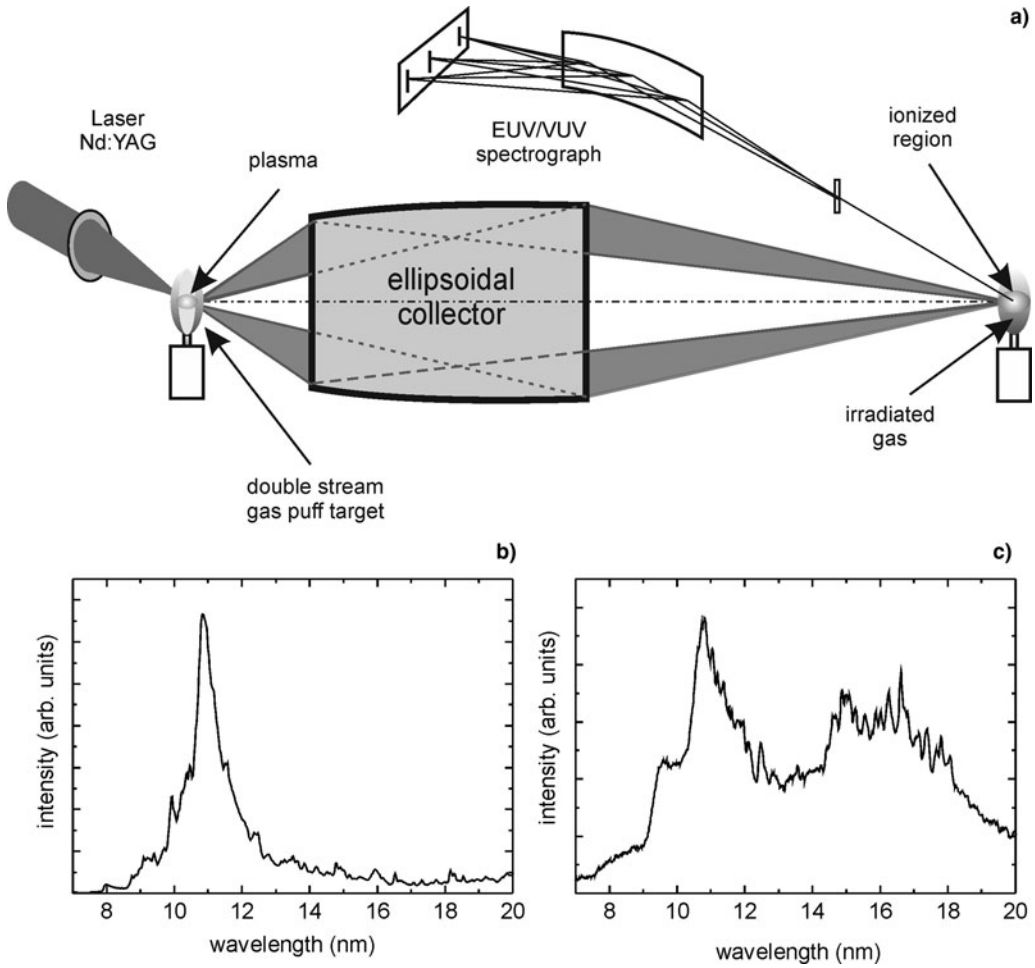

Fig. 1. Schematic view of the EUV Sources No. 1 and 2 indicating location of an auxiliary valve for gas injection into the interaction region, together with the EUV/VUV spectrograph (a) the EUV spectra of the focused radiation: Source No. 1 (b), Source No. 2 (c).

one of the mirrors which allows to form a parallel SXR/EUV beam that is focused by the second mirror. Spectrum of the focused radiation (Fig. 2c) is similar to the direct plasma emission spectrum (Fig. 2b); however, the relative intensity of the radiation close to 1 nm wavelength in comparison with the longer wavelengths is approximately two times lower. Maximum value of the SXR/EUV fluence in a focal plane of the collector reached 0.25 J/cm^2. Experimental arrangement of the source is shown in Figure 2a.

2.2. Gas Injection and Measurement Systems

EUV propagates only in vacuum, thus interaction of the EUV radiation with gases requires pulse injection of a gas stream into the vacuum chamber, synchronously with an SXR/EUV pulse. In our experiments, different gases were injected into the interaction region, perpendicularly to an optical axis of the irradiation system, using an auxiliary gas puff valve. The valve was equipped with a circular nozzle, having diameter of $\Phi = 0.7$ mm in case of the Source No. 1 and $\Phi =$ 2 mm in case of the other sources. An outlet of the nozzle was always located approximately 2.5 mm from the optical axis of the irradiating system. Larger nozzle diameter was allowed to increase the size of the interaction region and photoionized plasma. The larger plasma – the larger number of EUV photons emitted from the plasma. It enabled to minimize a number of laser pulses required for spectral measurements. The gas density in the interaction region was controlled by adjusting a gas backing pressure or the opening time of the valve. The density value was of the order of 1–10% of the atmospheric density.

Irradiation of gases injected into the interaction region, results in ionization and excitation of atoms and ions. The EUV spectra were measured using a grazing incidence, flat-field spectrometer (McPherson, Model 251), equipped with a 450 lines/mm toroidal grating. The spectral range of the spectrometer was $\lambda = 10$–95 nm. An optical axis of the spectrometer is perpendicular to the optical axis of the EUV or SXR irradiating system, thus the emission spectra are well separated from the spectra of the laser-plasma radiation. It is very important because the laser-plasma emission is approximately 10^5 times higher comparing with the photoionized plasma emission. The spectra, integrated over 10–500 pulses, were recorded using a charge-coupled device

https://doi.org/10.1017/S026303461500021X Published online by Cambridge University Press

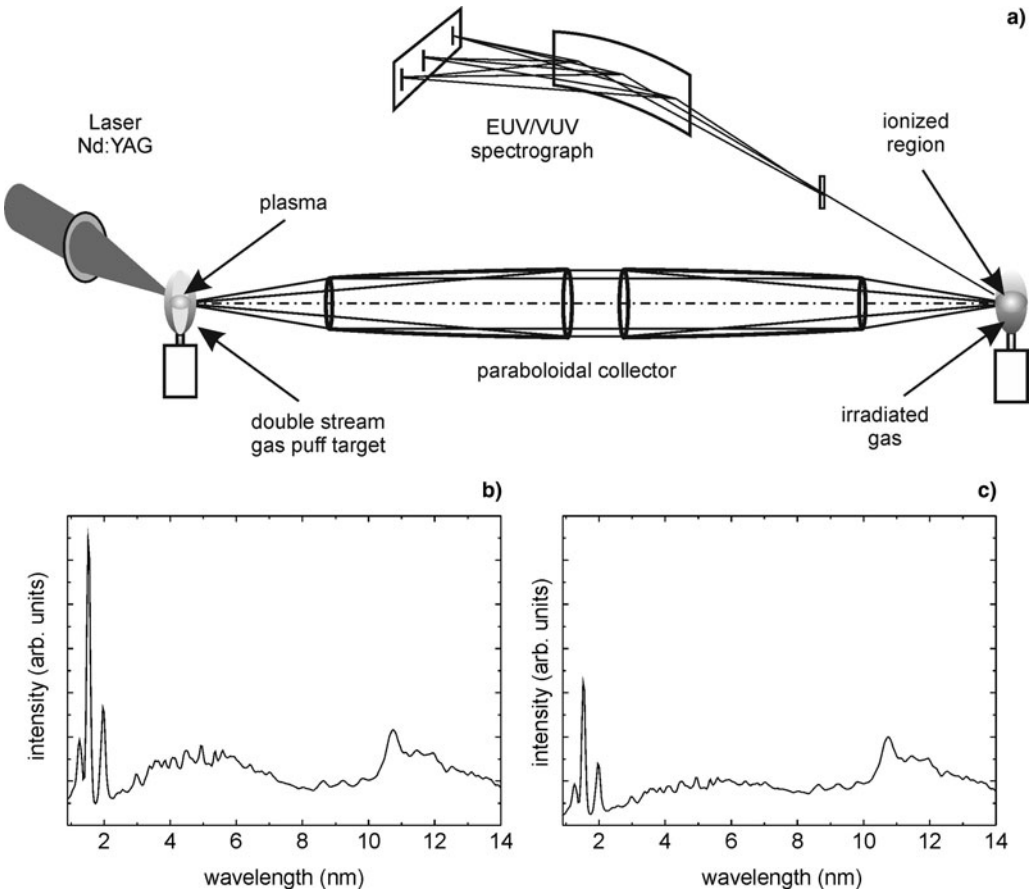

Fig. 2. Schematic view of the Source No. 3, indicating location of an auxiliary valve for gas injection into the interaction region, together with the EUV/VUV spectrograph (a) the SXR/EUV spectrum of direct plasma emission (b) and the SXR/EUV spectrum of the focused radiation (c).

detector, cooled down to a temperature of −40°C. A location of the auxiliary gas puff valve and the spectrograph in respect to the sources is depicted in Figures 1a and 2a.

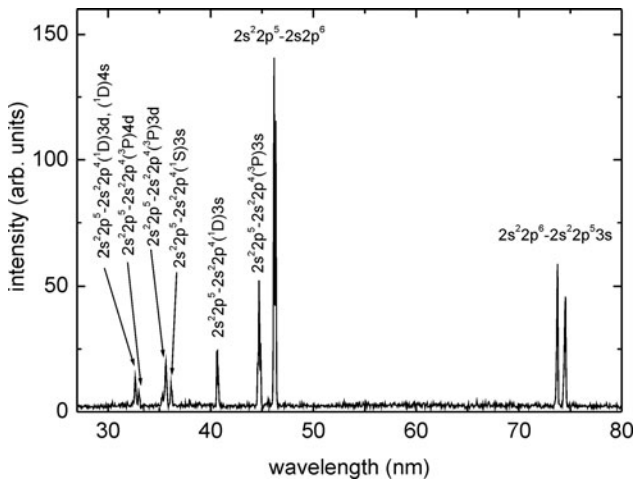

Fig. 3. A typical spectrum obtained for Ne photoionized plasmas using the irradiation system based on the Source No. 1.

3. EXPERIMENTAL RESULTS

Emission spectra, acquired for Ne photoionized plasmas using the irradiation systems, described in Section 2.1, are presented in Figures 3–5. The spectrum, depicted in Figure 3, was obtained by irradiation of Ne gas by the EUV pulses with relatively low fluence not exceeding 0.1 J/cm^2, using the Source No. 1. In this case, the spectra could be acquired for large number of pulses hence, despite low intensity of the emitted radiation, good quality spectra were obtained. The spectrum, shown in Figure 3, was obtained with 100 EUV pulses. It consists of multiple lines, originating from transitions in Ne atoms and singly charged Ne ions. The most intense line is a doublet corresponding to $2s^2 2p^5$–$2s2p^6$ transitions of Ne II ions. The spectrum was obtained for the gas density of the order of 10^{17} atoms/cm^3. Relative intensities of Ne II lines in case of higher densities remained practically unaltered. No lines corresponding to Ne III or higher ionization degrees were detected.

Significantly different are Ne spectra, depicted in Figure 4, obtained for the experimental arrangement employing the Source No. 2. Photoionized plasmas in this case were created by the EUV irradiation of Ne gas with much higher fluence

https://doi.org/10.1017/S026303461500021X Published online by Cambridge University Press

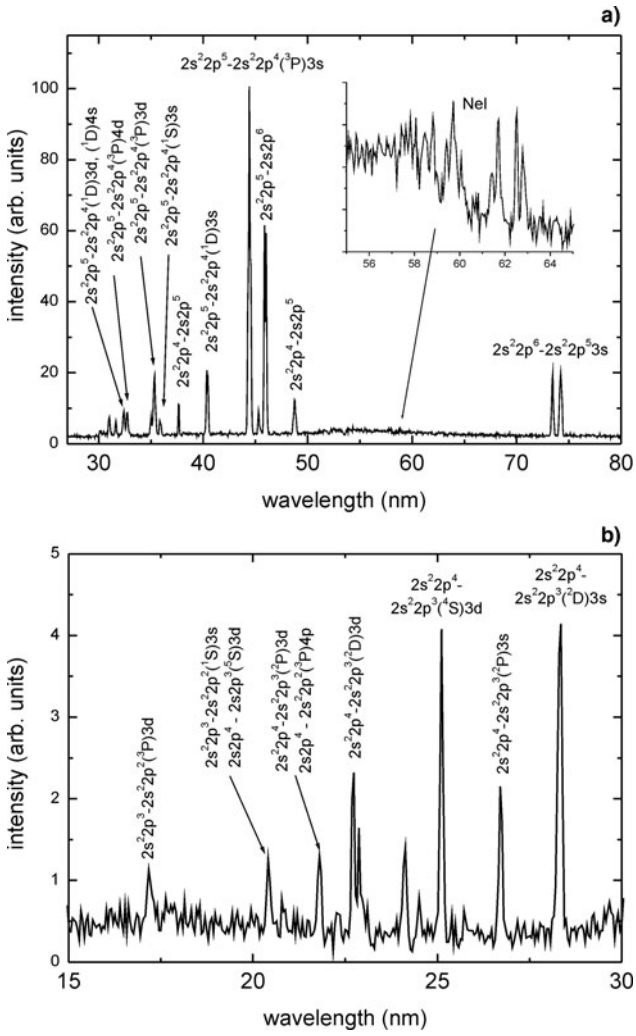

Fig. 4. A typical spectrum obtained for Ne photoionized plasmas using the irradiation system with the Source No. 2: (a) A long-wavelength range. (b) a short-wavelength range.

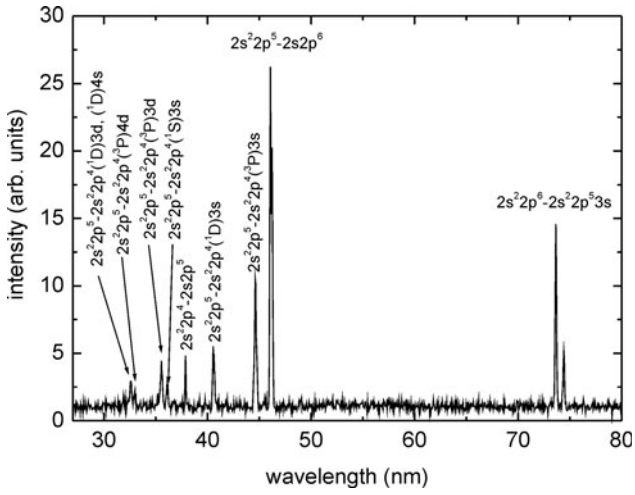

Fig. 5. A typical spectrum obtained for Ne photoionized plasmas using the irradiation system based on Source No. 3.

of approximately 0.4 J/cm^2. A single EUV exposure was limited to 10 pulses to avoid strong degradation of the gas puff nozzle exposed to hot plasmas. Despite a small number of EUV pulses, spectral intensities are comparable with the intensities obtained with hundreds of EUV pulses with the low fluence. It could be explained by higher EUV fluence and larger region of emission due to a larger nozzle outlet. As in the first case, the spectrum shown in Figure 3a consists of multiple lines, originating mainly from transitions in Ne atoms and singly charged Ne ions; however, it contains also well-pronounced spectral lines corresponding to $2s^22p^4$–$2s2p^5$ transition in Ne III ions at wavelengths of $\lambda = 37.9$ and $\lambda = 48.9$ nm. In this case, the $2s^22p^5$–$2s2p^6$ doublet of Ne II is not the most intense line. In fact, its intensity is almost two times lower comparing with the $2s^22p^5$–$2s^22p^4(^3P)3s$ line. Additional measurements performed in the shorter wavelength range revealed some weak spectral lines, shown in Figure 3b. The spectrum contains mainly lines corresponding to radiative transitions in NeIII ions; however, two of the lines originate from transitions in NeIV ions. These lines were not detected in case of using the Source No. 1.

The emission spectrum, presented in Figure 5, originates from photoionized plasmas, produced by the irradiation of Ne gas using the Source No. 3. Plasmas in this case were created by the SXR/EUV irradiation of the Ne gas with the fluence having intermediate value, between the values obtained from Sources No. 1 and 2. A single SXR/EUV exposure was limited to 25 pulses, again, to avoid strong degradation of the gas puff nozzle. The Ne spectrum is similar to that obtained in case of using the Source No. 1; however, there are two significant differences. First and the most important one is the presence of a clearly visible line corresponding to the $2s^22p^4$–$2s2p^5$ transition in Ne III ions, at the wavelength of $\lambda = 37.9$ nm. Its intensity is comparable with NeII lines, except the most intense $2s^22p^5$–$2s2p^6$ doublet. The second difference concerns two adjacent lines, corresponding to $2s^22p^6$–$2s^22p^53s$ transitions in neutral Ne atoms. Unlike the photoionized plasmas, produced using Sources No. 1 and 2, where relative intensities of these lines are almost the same, in case of employing the Source No. 3 their relative intensities differ approximately three times. No other lines, corresponding to Ne III or higher ionization degrees, were detected.

4. DISCUSSION

Ionization and excitation processes in Ne gas, driven by the EUV or SXR radiation, are significantly different comparing with plasma formation driven by IR lasers. In the latter case, assuming nanosecond Nd:YAG laser pulses for plasma creation, energy of a single irradiating photon is about 20 times lower than the ionization potential of Ne atoms. In this case, plasma is being heated due to inverse bremsstrahlung mechanism, reaching a high temperature, of the order of tens or even hundreds of eV, depending on the power density

https://doi.org/10.1017/S026303461500021X Published online by Cambridge University Press

of the laser beam. Energies of thermalized electrons are sufficiently high for ionization of atoms or even multicharged ions. In this case, collisional processes govern the ionization and excitation of atoms and ions. In such conditions, relative intensities of spectral lines are mainly associated with the ionization degree and electron temperature.

In case of irradiation of Ne gas with the EUV or SXR photons, direct photoionization of atoms or even ions by a single photon is possible. Apart from that, energies of the resulting photoelectrons are sufficiently high for further ionization or excitation. Additionally, due to quasi-continuous spectrum of the irradiating EUV/SXR photons, direct photoexcitation of different states is also possible. Radiative decay of the excited states results in a linear emission in a wide wavelength range, including the EUV range. In contrast to LPP, energy range of emitted photons is not strictly related to electron temperature. For the same reasons, there is no power density threshold to be exceeded for gas ionization or excitation. There is also no limitation for gas density; photoionized plasmas can be created in gases with very low densities, few orders of magnitude below atmospheric density.

Differences in spectral distributions, for Ne ions, indicated in Section 3, are associated with different irradiation conditions, in particular, with variety in radiation fluences and energies of the irradiating photons. In case of experimental arrangements utilizing Sources No. 1 and 2, energy range of the irradiating photons and maxima of the spectral distributions are similar. The significant difference concerns radiation fluences, over four times higher in case of using Source No. 2.

Taking into account relatively low intensity of irradiating photons and results of spectral measurements, indicating that mainly Ne^+ ions are produced, ion (or electron) density, created in all cases during the irradiation time, can be estimated from the equation:

$$\frac{dn_{Ne^+}}{dt} = (n_{Ne} - n_{Ne^+})\,\sigma_{ph,Ne^+} F \tag{1}$$

where n_{Ne+} is the density of singly charged Ne ions, n_{Ne} is the initial atomic density, (n_{Ne}−n_{Ne+}) is the current atomic density, $\sigma_{ph,Ne+}$ is the cross-section for photoionization of atoms, and F is the photon flux

Taking into account the experimental data for Source No. 1: $n_{Ne} = 10^{17}/\mathrm{cm}^3$, $F = 1.5\times10^{24}/\mathrm{cm}^2/\mathrm{s}$ and the photoionization cross-section (Samson & Stolte, 2002) $\sigma_{ph,Ne+} = 4\times10^{-18}\,\mathrm{cm}^2$, electron and singly charged ion density n_e,$n_{Ne+} = 2\times10^{15}/\mathrm{cm}^3$ can be obtained. In equation (1), recombination of Ne^+ ions was omitted because its rate, estimated based on the work by Pequignot *et al.* (1991), is over two orders of magnitude lower according to the photoionization rate. Average energies of the photoelectrons are sufficient for further ionization or excitations. Taking into account ionization potential of neutral atoms and average photon energy (approximately 100 eV), a single photoelectron, at best, can create three additional Ne^+ ions. Electron and ion densities in this case are still far below the initial atomic density, thus the estimation is reasonable. In case of the higher irradiation intensity, when using Source No. 2, it can be easily calculated that the electron (or n_{Ne+} ion) density is approximately four times higher.

Intensities of emission lines are determined by a time integration of the density of the excited ions multiplied by the spontaneous radiative decay rate. A significant difference in the emission spectra of photoionized plasmas concerns mainly relative intensities between $2s^22p^5$–$2s2p^6$ and $2s^22p^5$–$2s^22p^4$3l lines. To explain this difference we can consider the $2s^22p^5$–$2s^22p^4(^3\mathrm{P})3s$ transition. Density of the $2s^22p^4(^3\mathrm{P})3s$ state can be obtained from the equation:

$$\frac{dn_2}{dt} = n_1\, n_e \langle \sigma_{e,12}\, v\rangle - n_2\, A_{21} \tag{2}$$

where:$n_1$is the density of singly charged Ne ions in the ground state, n_2 is the density of Ne ions in the $2s^22p^43s$ excited state, $\sigma_{e,12}$ is the cross-section for the electron impact excitation to the $2s^22p^43s$ state, v is the electron speed, A_{12} is the rate of spontaneous emission for the $2s^22p^43s$ – $2s^22p^5$ transition.

An equation for density of the $2s2p^6$ state should contain additionally a contributing factor concerning photoionization from the $2s$ shell. In this case, the equation can be expressed as:

$$\frac{dn_3}{dt} = (n_{Ne} - n_{Ne^+})\,\sigma_{ph,3}\, F + n_1\, n_e \langle \sigma_{e,13}\, v\rangle - n_3\, A_{31} \tag{3}$$

where n_3 is the density of Ne ions in the $2s2p^6$ excited state, $\sigma_{ph,3}$ is the cross-section for photoionization of atoms to the $2s2p^6$ excited state, $\sigma_{e,13}$ is the cross-section for electron impact excitation to the $2s2p^6$ excited state, and A_{31} is the rate of spontaneous emission for the $2s2p^6$–$2s^22p^5$ transition.

In both the cases, the electron impact deexcitation can be neglected due to low electron and ion densities. It should be also pointed out that the electron impact excitation cross-sections (Griffin *et al.*, 2001) and spontaneous radiative decay rates (Verner *et al.*, 1996) for both the states have similar values. In this case, relative intensities of the $2s^22p^5$–$2s2p^6$ and $2s^22p^5$–$2s^22p^43s$ lines will be strongly influenced by the term (n_{Ne}−n_{Ne+}) $\sigma_{ph,3}F$. Its value decreases with time due to decrease of neutral atoms density. Simultaneously the term $n_1\, n_e\langle\sigma_{e,13}\, v\rangle$ increases as n_e^2. Taking into account the corresponding cross-section for the inner-shell photoionization (Samson & Stolte, 2002), its value, in case of using the Source No. 1, can be estimated to be $6\times10^{22}/\mathrm{cm}^3/\mathrm{s}$. For obvious reasons this term is dominating at the beginning of the irradiation process, however, during the irradiation electron and Ne^+ ion densities increase and finally the collisional term reaches a comparable value to the photoionization term. In case of using the Source No. 2 for the creation of the photoionized plasma, the photoionization term reaches the value approximately four times higher

https://doi.org/10.1017/S026303461500021X Published online by Cambridge University Press

comparing with the Source No. 1. Simultaneously, however, the collisional term reaches even ten times higher value, which means that this term becomes dominating. It can be thus concluded that relative decrease of the emission line, corresponding to the $2s^2 2p^5$–$2s2p^6$ transition, is associated with a significant increase of the collisional excitation over inner-shell ionization.

Higher fluence of the EUV radiation pulses, in case of using the Source No. 2, results also in presence of Ne III and even Ne IV ions. The corresponding lines emitted in the shorter wavelength range are presented in Figure 4b. Their intensities are over 20 times smaller comparing with the most intense lines from Figure 4a. There are, however, also more intense Ne III lines corresponding to $2s^2 2p^4$–$2s2p^5$ transitions, clearly visible in the long wavelength range. Their relatively high intensity is again associated with significant contribution of the inner-shell photoionization, this time in Ne^+ ions. None of these lines was detected in case of using Source No. 1 for the photoionized plasma creation.

The spectrum obtained from Ne plasma produced using Source No. 3 is similar to the spectrum obtained using Source No. 1. In both the cases emission lines originating from Ne II ions have practically the same relative intensities. On the other hand, the spectrum contains a single Ne III line corresponding to $2s^2 2p^4$–$2s2p^5$ transition at the wavelength of $\lambda = 37.9$ nm; however, it does not contain any other Ne III lines. Excitation to the $2s2p^5$ state can be again associated with the inner-shell photoionization; however, it can be also caused by the inner-shell ionization by electrons with high energy, up to 1 keV, not present in case of using the two other sources. Two adjacent lines at $\lambda = 73.6$ and 74.4 nm originating from neutral neon atoms, correspond to a resonance and intercombination transitions, respectively. Their intensity ratio in coronal equilibrium, which is valid for low-density plasmas, should be proportional to the ratio of the corresponding electron impact excitation rates. This ratio in the wide energy range has the value of 3–5 (Tsurubuchi *et al*., 2000), which corresponds to the value obtained in the experiment. It would suggest that in case of these transitions the collisional excitation is dominating. However, in case of the two other sources this ratio is more or less equal to 1. Reasons of this difference remain unclear.

5. SUMMARY

In this paper, first results of comparative investigations, concerning photoionized Ne plasmas created using laser-plasma-produced EUV and SXR sources of different parameters, are presented. Significant differences between experimental configurations concerning the irradiation conditions are indicated. In all cases, the EUV emission spectra of the excited atoms and singly charged Ne ions were registered. The most important differences between the spectra concern relative intensities of the $2s^2 2p^5$–$2s2p^6$ doublet in respect to the other Ne II lines and also relative intensities of two adjacent lines, corresponding to $2s^2 2p^6$–$2s^2 2p^5 3s$ transitions in neutral atoms. Apart from that, in case of the experimental configuration with the highest fluence, multiple lines corresponding to doubly and even triply charged ions were detected. Atomic processes, dominating in photoionized plasmas obtained for different irradiation conditions, were analyzed. It was concluded that significant differences in relative intensities of the spectral lines are associated with different contributions of the inner-shell photoionization and collisional excitation to population distribution of the excited states during the process of photoionized plasma formation.

ACKNOWLEDGMENTS

This work was supported by the grant UMO-2013/09/B/ST2/01625 of the National Science Centre, Poland, by the European Commission's Seventh Framework Program (LASERLAB-EUROPE) and by EU from EUROPEAN REGIONAL DEVELOPMENT FUND, project number: WND – POiG.02.01.00 – 14 – 095/09.

REFERENCES

Bailey, J.E., Cohen, D., Chandler, G., Cuneo, M., Foord, M., Heeter, R., Jobe, D., Lake, P., Liedahl, D., MacFarlane, J., Nash, T., Nielson, D., Smelser, R. & Stygar, W. (2001). Neon photoionization experiments driven by Z-pinch radiation. *J. Quantum Spectrosc. Radiat. Transf.* **71**, 157.

Bartnik, A., Fiedorowicz, H., Jarocki, R., Juha, L., Kostecki, J., Rakowski, R. & Szczurek, M. (2005). Micromachining of organic polymers by X-ray photo-etching using a 10 Hz laser-plasma radiation source. *Microelectron. Eng.* **78–79**, 452–456.

Bartnik, A., Fiedorowicz, H., Jarocki, R., Kostecki, J., Szczurek, M. & Wachulak, P.W. (2011). Laser-plasma EUV source dedicated for surface processing of polymers. *Nucl. Inst. Methods Phys. Res. A* **647**, 125–131.

Bartnik, A., Fedosejevs, R., Wachulak, P., Fiedorowicz, H., Serbanescu, C., Saiz, E.G., Riley, D., Toleikis, S. & Neely, D. (2013*a*). Photo-ionized neon plasmas induced by radiation pulses of a laser-plasma EUV source and a free electron laser FLASH. *Laser Part. Beams* **31**, 195–201.

Bartnik, A., Wachulak, P., Fiedorowicz, H., Fok, T., Jarocki, R. & Szczurek, M. (2013*b*). Detection of significant differences between absorption spectra of neutral helium and low temperature photoionized helium plasmas. *Phys. Plasmas* **20**, 113302.

Bartnik, A., Wachulak, P., Fiedorowicz, H., Jarocki, R., Kostecki, J. & Szczurek, M. (2013*c*). Luminescence of He and Ne gases induced by EUV pulses from a laser plasma source. *Radiat. Phys. Chem.* **93**, 9–14.

Cohen, D.H., MacFarlane, J.J., Bailey, J.E. & Liedahl, D.A. (2003). X-ray spectral diagnostics of neon photoionization experiments on the Z-machine, Rev. *Sci. Instrum.* **74**, 1962.

Fujioka, S., Takabe, H., Yamamoto, N., Salzmann, D., Wang, F., Nishimura, H., Li, Y., Dong, Q., Wang, S., Zhang, Y., Rhee, Y., Lee, Y., Han, J., Tanabe, M., Fujiwara, T., Nakabayashi, Y., Zhao, G., Zhang, J. & Mima, K. (2009). X-ray astronomy in the laboratory with a miniature compact object produced by laser-driven implosion. *Nat. Phys.* **5**, 821–825.

Gallagher, J.W., Brion, C.E., Samson, J.A.R. & Langhoff, P.W. (1988). Absolute cross sections for molecular photoabsorption,

https://doi.org/10.1017/S026303461500021X Published online by Cambridge University Press

partial photoionization, and ionic photofragmentation processes. *J. Phys. Chem. Ref. Data* **17**, 9–153.

Griffin, D.C., Mitnik, D.M. & Badnell, N.R. (2001). Electron-impact excitation of Ne+. *J. Phys. B: At. Mol. Opt. Phys.* **34**, 4401–4415.

Hurricane, O.A., Callahan, D.A., Casey, D.T., Celliers, P.M., Cerjan, C., Dewald, E.L., Dittrich, T.R., Doppner, T., Hinkel, D.E., Berzak Hopkins, L.F., Kline, J.L., Le Pape, S., Ma, T., MacPhee, A.G., Milovich, J.L., Pak, A., Park, H.-S., Patel, P.K., Remington, B.A., Salmonson, J.D., Springer, P.T. & Tommasini, R. (2014). Fuel gain exceeding unity in an inertially confined fusion implosion. *Nature* **506**, 343–348.

Itikawa, Y., Ichimura, A., Onda, K., Sakimoto, K., Takayanagi, K., Hatano, Y., Hayashi, M., Nishimura, H. & Tsurubuchi, S. (1989). Cross sections for collisions of electrons and photons with oxygen molecules. *J. Phys. Chem. Ref. Data* **18**, 23–42.

Juha, L., Krasa, J., Cejnarova, A., Chvostova, D., Vorlicek, V., Krzywinski, J., Sobierajski, R., Andrejczuk, A., Jurek, M., Klinger, D., Fiedorowicz, H., Bartnik, A., Pfeifer, M., Kubat, P., Pina, L., Kravarik, J., Kubes, P., Bakshaev, Y.L., Korolev, V.D., Chernenko, A.S., Ivanov, M.I., Scholz, M., Ryc, L., Feldhaus, J., Ullschmied, J. & Boody, F.P. (2003). Ablation of various materials with intense XUV radiation. *Nucl. Instrum. Methods A* **507**, 577.

Lammer, H., Eybl, V., Kislyakova, K.G., Weingrill, J., Holmström, M., Khodachenko, M.L., Kulikov, Yu.N., Reiners, A., Leitzinger, M., Odert, P., Xiang Grüß, M., Dorner, B., Güdel, M. & Hanslmeier, A. (2011). UV transit observations of EUV-heated expanded thermospheres of Earth-like exoplanets around M-stars: Testing atmosphere evolution scenarios, Astrophys. *Space Sci.* **335**, 39–50.

Makimura, T., Kenmotsu, Y., Miyamoto, H., Niino, H. & Murakami, K. (2005). Ablation of silica glass using pulsed laser plasma soft X-rays. *Surf. Sci.* **593**, 248–251.

Mancini, R.C., Bailey, J.E., Hawley, J.F., Kallman, T., Witthoeft, M., Rose, S.J. & Takabe, H. (2009). Accretion disk dynamics, photoionized plasmas, and stellar opacities. *Phys. Plasmas* **16**, 041001.

Pequignot, D., Petitjean, P. & Boisson, C. (1991). Total and effective radiative recombination coefficients. *Astron. Astrophys.* **251**, 680–688.

Perry, T.S., Springer, P.T., Fields, D.F., Bach, D.R., Serduke, F.J.D., Iglesias, C.A., Rogers, F.J., Nash, J.K., Chen, M.H., Wilson, B.G., Goldstein, W.H., Rozsynai, B., Ward, R.A., Kilkenny, J.D., Doyas, R., Da Silva, L.B., Back, C.A., Cauble, R., Davidson, S.J., Foster, J.M., Smith, C.C., Bar-Shalom, A. & Lee, R.W. (1996). Absorption experiments on x-ray-heated mid-Z constrained samples. *Phys. Rev. E* **54**, 5617–5631.

Samson, J.A.R. & Stolte, W.C. (2002). Precision measurements of the total photoionization cross-sections of He, Ne, Ar, Kr, and Xe. *J. Electron Spectrosc. Relat. Phenom.* **123**, 265–276.

Tsurubuchi, S., Arakawa, K., Kinokuni, S. & Motohashi, K. (2000). Electron-impact cross sections of Ne. *J. Phys. B: At. Mol. Opt. Phys.* **33**, 3713–3723.

Verner, D.A., Verner, E.M. & Ferland, G.J. (1996). Atomic data for permitted resonance lines of atoms and ions from H to Si, and S, Ar, Ca, and Fe. *At. Data Nucl. Data Tables* **64**, 1–180.

Watson, W.S. (1972). Photoionization of helium, neon and argon in the 60–230 eV photon energy range. *J. Phys. B: At. Mol. Phys.* **5**, 2292–2303.

Wei, H.G., Shi, J.R., Zhao, G., Zhang, Y., Dong, Q.L., Li, Y.T., Wang, S.J., Zhang, J., Liang, Z.T., Zhang, J.Y., Wen, T.S., Zhang, W.H., Hu, X., Liu, S.Y., Ding, Y.K., Zhang, L., Tang, Y.J., Zhang, B.H., Zheng, Z.J., Nishimura, H., Fujioka, S., Wang, F.L. & Takabe, H. (2008). Opacity studies of silicon in radiatively heated plasmas. *Astrophys. J.* **683**, 577–583.

Zhang, Y., Katoh, T., Washio, M., Yamada, H. & Hamada, S. (1995). High aspect ratio micromachining Teflon by direct exposure to synchrotron radiation. *Appl. Phys. Lett.* **67**, 872.

https://doi.org/10.1017/S026303461500021X Published online by Cambridge University Press